RSC Advances

RSCPublishing

ARTICLE

Hydrogen-bond-assisted isotactic-specific radical polymerization of *N*-vinyl-2-pyrrolidone with tartrate additives in toluene at low temperatures: high-resolution ^{1}H NMR analysis

Cite this: DOI: 10.1039/x0xx00000x

Received 00th January 2012,
Accepted 00th January 2012

DOI: 10.1039/x0xx00000x

www.rsc.org/

Tomohiro Hirano*, Yuya Miyamoto, Shinya Amano, Kazuya Tatsumi, Takuya Anmoto, Hiroshi Kimura, Ken Yoshida, Miyuki Oshimura and Koichi Ute

A diethyl L-tartrate (L-EtTar)-assisted radical polymerization of *N*-vinyl-2-pyrrolidone has been developed as the first reported example of the synthesis of isotactic-rich poly(*N*-vinyl-2-pyrrolidone) (PVP). The addition of L-EtTar in toluene at temperatures of −40°C and lower led to a significant increase in the polymer yield by one order of magnitude compared with the reaction in the absence of L-EtTar. Decreasing the polymerization temperature led to increases in the isotacticity of the PVP, with the *mm* triad reaching 66.4% at −93 °C. ^{1}H NMR measurement at 920 MHz was conducted to establish a reliable strategy for quantifying the triad tacticities. High-temperature NMR measurements at 250 °C were performed using a specially-designed NMR probe, which led to dramatic narrowing of the ^{1}H line width.

Introduction

Poly(*N*-vinyl-2-pyrrolidone) (PVP) has been used extensively in numerous applications in the pharmaceutical, cosmetic and food industries.[1-6] The development of new methods for the synthesis of PVP are highly desired to provide better control over its physical properties by allowing for the tuning of its stereoregularity over a wide range of tacticities. However, progress in this area has been severely limited, because radical polymerization is the only method of polymerization that is currently available for the synthesis of PVP. Controlling the stereospecificity in the radical polymerization of vinyl monomers, especially unconjugated monomers, can be particularly challenging because the high reactivity of the terminal radicals overwhelms the orientational preference of the incoming monomers.[7-13] Based on these limitations, there have been very few reports pertaining to the stereoregularity of PVP.[14-21] An alternative approach to this problem involves the use of cationic polymerization, although this approach generally affords PVP with such a low molecular weight that it would be more appropriately categorized as an oligomer.

We recently reported that the stereospecificity of low-temperature radical polymerizations could be finely tuned by taking advantage of the hydrogen-bond-assisted complex formation between amide-containing vinyl monomers and alcohol compounds at low temperatures.[10,22-26] Of the alcohol compounds examined to date, tartrates exhibited a unique ability to regulate the stereochemistry during the polymerization of monomers bearing amide group through the formation of complexes based on double hydrogen-bonding interactions. For example, tartrates induced syndiotactic specificity in the radical polymerization of *N*,*N*-dimethylacrylamide (DMAAm) in toluene at low temperatures,[25, 27] whereas the polymerization reaction conducted under the same conditions without tartrates afforded isotactic-rich polymers.[28] In contrast, the addition of tartrates to the radical polymerization of the unconjugated monomer *N*-vinylacetamide (NVA) in toluene at −60 °C gave isotactic-rich polymers with an *mm* triad of up to 49%.[10] Furthermore, the yields of the polymers increased for both conjugated and unconjugated monomers when tartrates were added to the radical polymerization reactions at low temperatures.[10,25] In this study, we shall investigate whether the addition of tartrates can lead to a dramatic improvement in the efficiency of the polymerization of *N*-vinyl-2-pyrrolidone (VP) at low temperatures, where the hydrogen bonding interactions are rigid enough to allow for more strict stereochemical control over the radical propagation of VP. In order to uncover the evidence of the formation of a hydrogen-bonding complex between VP and L-EtTar, here we attempt to verify the changes in the NMR spectra of these compounds when they came into contact with each other. We shall discuss the mechanism for the induced isotactic specificity in terms of the activation free energies for the isotactic and syndiotactic propagation steps.

One of the important objectives of this study is to provide, the renewed assignments for the ^{1}H NMR spectra of PVP that can be used to determine the tacticity of this newly-synthesized PVP. To establish the new assignments, we systematically

examined the optimal solvent and temperature conditions for the NMR measurement, and these conditions will be discussed in greater detail below. Because the ^{13}C spectrum has been used more often in the NMR studies on PVP, we briefly compare the new assignments for the ^{1}H spectra with those of the earlier assignments based on the ^{13}C spectra of PVP.[14,17] To validate our new ^{1}H NMR assignment and to confirm its quantitative precision, ultra-high-field NMR measurements at ^{1}H frequencies of 920 MHz was performed. It is noteworthy that NMR measurements over a wide range of tacticities have allowed us to distinguish more clearly between the peaks for different stereosequences.

In an attempt to achieve further improvements in the resolution and separability of the NMR signals, we also investigated the advantages of running high-temperature NMR measurement in subcritical fluids at temperatures up to 250 °C in the first reported application of an NMR probe that was specially-designed for high-temperature measurements.[29] One of the major difficulties encountered during NMR studies on polymers results from signal broadening, which occurs as a consequence of the slowing down of the molecular motion and the severe overlap of signals assigned to different stereosequences. The aim of the present study is, therefore, to explore the extent to which the accelerated motions of both the main chain and side chain would narrow and simplify the NMR peaks obtained at such extremely high temperatures. We investigated the effect of the solvents using protic, hydrophobic aprotic and amphiphilic aprotic solvents (i.e., D_2O, $CDCl_3$ and DMSO-d_6, respectively) to assess the peak separation and splitting in different solvents. This study therefore represents a big step forward with respect to the development of high-temperature NMR methods from simple pure-solvent systems involving small molecules[29-33] towards macromolecular systems with elaborate control over the stereochemistry.

Experimental

Materials

VP (Wako Pure Chemical Industries, Osaka, Japan, ≥98%) was purified by fractional distillation. Toluene (Kanto Chemical, Tokyo, Japan, ≥99.0%) was washed sequentially with sulphuric acid, water and 5% aqueous NaOH, and then further purified by fractional distillation. A solution of tri-*n*-butylborane (*n*-Bu_3B) in tetrahydrofuran (THF) (1.0 mol L^{-1}), toluene-d_8 containing 1 v/v% tetramethylsilane (TMS), 3-(trimethylsilyl)propanesulfonic acid (TMSPS) (97%) (Sigma-Aldrich Japan, Tokyo, Japan), diethyl ether (≥99.0%), DMSO-d_6 containing 0.05 v/v% TMS, D_2O (Wako Pure Chemical Industries), chloroform-*d* containing 0.03 v/v% TMS (Merck Ltd. Japan, Tokyo, Japan), 2,6-di-*t*-butyl-4-methylphenol (≥99.0%), L-EtTar (≥98.0%) (Tokyo Chemical Industry, Tokyo, Japan) *N*,*N*-dimethylformamide (Kanto Chemical, HPLC grade, ≥99.7%) and LiBr (Kishida Chemical, Osaka, Japan, anhydrous ≥95%) were used as received.

Polymerization

A typical polymerization procedure was conducted as follows. VP (1.170 g, 10.5 mmol) and L-EtTar (2.175 g, 10.5 mmol) were dissolved in toluene to give a 10 mL solution ($[VP]_0$ = $[L\text{-}EtTar]_0$ = 1.05 mol L^{-1}). Nine milliliters of the solution was transferred to a glass ampoule and placed into a methanol bath thermostated at a reaction temperature in Table 1. The polymerization was initiated by adding 0.47 mL of a *n*-Bu_3B solution in THF to the mixture in the glass ampoule under air, and the resulting solution was held for 24 h at a constant temperature. The *n*-Bu_3B is known as a low temperature initiator which provides alkyl radical via formation of peroxide.[34] The reaction was terminated with the addition of a 0.5 mL solution of 1.0 mol L^{-1} 2,6-di-*t*-butyl-4-methylphenol in THF at the polymerization temperature. The polymerization mixture was then poured into diethyl ether (1 L) to precipitate the product polymer, and the precipitate was collected by centrifugation and dried *in vacuo* at 60 °C for 48 h. The polymer yield was determined gravimetrically.

Size exclusion chromatographic measurement

The relative molecular weights and molecular weight distributions of the polymers were determined by size exclusion chromatography (SEC) using polystyrene samples as molecular weight standards.[35-37] SEC was performed on an HLC 8220 chromatographic instrument (Tosoh, Tokyo, Japan), equipped with TSK gel columns [SuperHM-M (150 × 6.5 mm, i.d.) and SuperHM-H (150 × 6.5 mm, i.d.)] (Tosoh). Dimethylformamide containing 10 mmol L^{-1} LiBr was used as the eluent at 40 °C and a flow rate of 0.35 mL min^{-1}. The initial polymer concentration was set at 1.0 mg mL^{-1}.

NMR measurement

^{1}H NMR spectra were recorded on EX-400, ECA-400, ECA-500 spectrometers (JEOL, Tokyo, Japan) at the University of Tokushima and on ECA-920 one (JEOL) at Institute for Molecular Science, Japan, all of which are equipped with 5-mm standard multinuclear direct detection probes. The high-temperature ^{1}H NMR spectra were recorded on the ECA-500 spectrometer using a high-temperature probe, which was developed by one of the authors (KY).[29] The sample solution was sealed in a quartz tube as described elsewhere.[29] The proton chemical shifts of the polymers in D_2O (99.9% atom D) at temperatures up to 84 °C were referenced to the methyl groups of TMSPS (δ = 0.017 ppm), which was used as an internal reference.[38] TMSPS was not used as an internal reference for the high temperature NMR measurements in D_2O because of concerns over side reactions including decomposition of the PVP. In these cases, the middle methylene groups (*cf.* Fig. 1, **d**) of the trimethylene groups on the side chain (δ = 2.058 ppm) of the polymer were used as a proton-chemical-shift reference. The proton chemical shifts of polymers in $CDCl_3$ (99.8% atom D) and DMSO-d_6 (99.9% atom D) were referenced to internal TMS (i.e., δ = 0.000 ppm) and the residual non-deuterated solvent peak in DMSO-d_6 (i.e., δ = 2.500 ppm), respectively. The proton and carbon chemical shifts of VP and L-EtTar in toluene-d_8 (99.5% atom D) were reference to internal TMS (i.e., δ = 0.000 ppm).

Results and discussion

^{1}H NMR assignments of triad stereosequences

Let us begin by examining the ^{1}H NMR spectra of the PVPs synthesized in the presence of L-EtTar at different temperatures. A comparison of the spectra for the polymer samples prepared at polymerization temperatures of 0 and −90 °C is shown in Table 1, where the details of the different samples are listed as

runs 6 and 12, respectively. The lower temperature of −90 °C is only 5 °C higher than the melting point of toluene. The ^{1}H NMR spectra of the two different samples were measured in both D_2O and $CDCl_3$, and the resulting four spectra are shown in Fig. 1.

We initially considered the signals of the main-chain methylene groups (denoted as $CH_{2,main}$, **a**, in Fig. 1). The ^{1}H NMR signals of the atomic sites on the main-chain methylene groups of vinyl polymers can be used to provide conclusive information about the diad tacticities of the polymers. For example, the protons in a meso (*m*) diad give two separate peaks because of the magnetic non-equivalence of the protons placed in an antisymmetric manner along the main chain. In contrast, the protons in a racemo (*r*) diad give a single peak because of the rotational symmetry. There were clear differences in the $CH_{2,main}$ peaks (**a**) in the ^{1}H NMR spectra of the polymers synthesized at the high and low temperatures when the spectra were measured in $CDCl_3$. Three $CH_{2,main}$ peaks were observed in the spectrum of the polymer prepared at the higher temperature of 0 °C (Fig. 1, upper right), including the one in the middle (indicated with an arrow), which was observed as a shoulder. In contrast, the ^{1}H NMR spectrum of the sample prepared at the lower temperature of −90 °C (Fig. 1, lower right) only contained two peaks for the $CH_{2,main}$ group. The chemical shift values of the two peaks coincided with the two major peaks of the three, as shown in the upper right panel of Fig. 1, and the center peak was almost absent from the lower right panel. Following the principle mentioned above concerning the relationship between the multiplicity of the NMR signals and the symmetry of the diad stereochemistries, the center peak can be assigned to the *r* diad, and the two peaks on either side of the center peak can be assigned to the *m* diad. In this way, it is possible to confirm that the sample prepared at −90 °C was richer in the *m* diad than the sample prepared at 0 °C. It is noteworthy that the separation between the center peak for *r* diad and the side peaks for the *m* diad was only observed in $CDCl_3$. These peaks were not observed in the ^{1}H NMR spectra of the samples measured in D_2O (left panels of Fig. 1), therefore highlighting the importance of choosing the appropriate solvent for evaluating the NMR signals of interest.

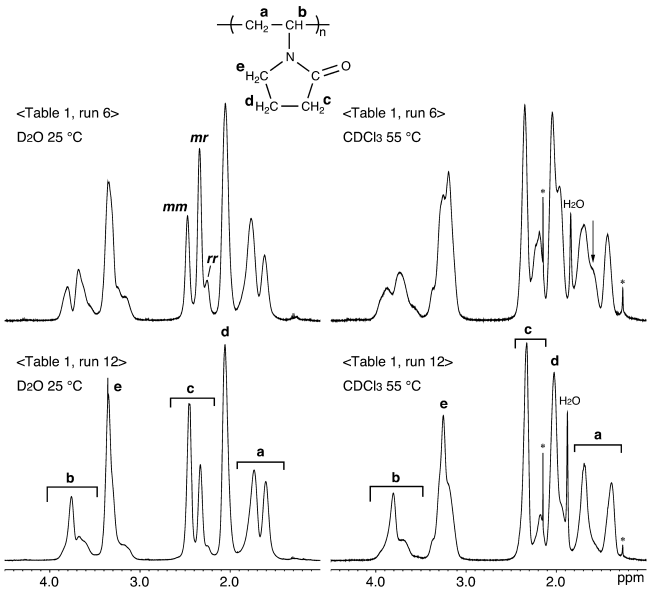

Fig. 1 500 MHz ^{1}H NMR spectra of PVPs with different tacticities, measured in D_2O at 25 °C (left panel) and $CDCl_3$ at 55 °C (right panel). The sharp peaks with asterisk (*) are impurities.

Now, let us move on to the proton signals of the side chains. The signals of the side-chain groups reflect odd-number stereosequences, such as triad and pentad sequences, with the former of these two sequences having the more dominant effect. For the purpose of determining the triad tacticities, we focused on the proton signals of the methylene group adjacent to the C=O group of the side chain ($CH_{2,C=O}$, **c**) in the spectra measured in D_2O, because these signals were clearly separated into three distinct peaks (Fig. 1, upper and lower left). These three peaks were subsequently assigned to triad stereosequences of *mm*, *mr* and *rr* from the low to the high magnetic field, as indicated in Fig. 1. The peak at the lowest magnetic field was assigned to the *mm* stereosequence, because this peak was larger for the sample prepared at −90 °C (lower left), which was determined to be rich in the *m* diad based on its $CH_{2,main}$ signal, as described above. The question is then narrowed down to assigning the other two peaks for the *mr* and *rr* stereosequences.

Table 1. Radical polymerization reactions of VP in toluene at low temperatures for 24 h in the presence or absence of L-EtTar, average lengths of the *m* diad ($\bar{n}_m$) of the polymers obtained and first order Markovian parameters for the polymerizations[a]

Run	$[VP]_0$ / mol L^{-1}	$[L\text{-EtTar}]_0$ / mol L^{-1}	Temp. / °C	Yield / %	$M_n \times 10^{-3}$ [b]	M_w/M_n [b]	Triad tacticity[c] / %			$\bar{n}_m$ [d]	Markovian Parameters		
							f_{mm}	f_{mr}	f_{rr}		$P_{m/r}$ [e]	$P_{r/m}$ [f]	$P_{m/r} + P_{r/m}$
1	2.0	0.0	0	66	7.2	2.5	42.8	49.8	8.4	2.68	0.368	0.748	1.116
2	1.0	0.0	0	48	4.4	2.4	43.1	48.9	8.0	2.76	0.362	0.753	1.115
3[g]	1.0	0.0	–20	14	4.2	1.4	46.2	46.3	7.5	3.00	0.334	0.755	1.089
4[g]	1.0	0.0	–40	3	n.d.[h]	n.d.[h]	n.d.[h]	n.d.[h]	n.d.[h]	n.d.[h]	n.d.[h]	n.d.[h]	n.d.[h]
5[g]	1.0	0.0	–60	0	-	-	-	-	-	-	-	-	-
6	2.0	2.0	0	81	10.9	2.6	34.0	53.6	12.4	2.27	0.441	0.684	1.125
7	1.0	1.0	0	70	5.9	2.5	36.3	53.7	10.0	2.35	0.425	0.729	1.154
8	1.0	1.0	–20	43	6.6	2.6	39.4	51.7	8.9	2.53	0.396	0.744	1.140
9	1.0	1.0	–40	51	7.5	2.3	43.9	48.9	7.2	2.80	0.358	0.773	1.131
10	1.0	1.0	–60	51	10.7	2.0	51.1	43.5	5.4	3.35	0.299	0.801	1.100
11	1.0	1.0	–80	35	n.d.[h]	n.d.[h]	60.1	36.4	3.5	4.31	0.232	0.839	1.071
12	1.0	1.0	–90	35	n.d.[h]	n.d.[h]	62.1	35.2	2.7	4.53	0.221	0.867	1.088
13	1.0	1.0	–93	6	n.d.[h]	n.d.[h]	66.4	31.9	1.7	5.17	0.194	0.904	1.098

[a] $[n\text{-}Bu_3B]_0 = 5.0 \times 10^{-2}$ mol L^{-1}. [b] Determined by SEC. [c] Determined by ^{1}H NMR. [d] $\bar{n}_m = (f_{mm} + f_{mr}/2) / (f_{mr}/2)$. [e] $P_{m/r} = (f_{mr}/2) / (f_{mm} + f_{mr}/2)$. [f] $P_{r/m} = (f_{mr}/2) / (f_{rr} + f_{mr}/2)$. [g] For 48 h. [h] Not determined.

To assign these stereosequences, we focused on the statistical probabilities of different diad tacticities for the propagation of the polymer. For radical polymerization reactions, the stereosequences of the polymers obey simple Bernoullian statistics in most cases, and the polymer synthesized in the current study was also found to follow Bernoullian statistics, as described below. According to Bernoullian statistics, each step in the propagation of the polymer is independent of the preceding propagation step, and the fractions the of *mr* and *rr* triads, denoted respectively as f_{mr} and f_{rr}, in the final product polymer can be calculated with the stepwise probability of the generation of *m* and *r* diads, respectively, which are denoted as P_m and P_r (= 1–P_m). Thus the fractions f_{mr} and f_{rr} are obtained in terms of P_m as $f_{mr} = 2P_m(1–P_m)$ and $f_{rr} = (1–P_m)^2$. The probability P_m is equal to the square root of the fraction f_{mm} in Bernoullian statistics, and the fraction f_{mm} can be experimentally obtained from the ^{1}H NMR spectra because the peak for the *mm* triad has already assigned, as described above. In other words, once f_{mm} has been determined experimentally, it is possible to calculate f_{mr} and f_{rr} based on the assumptions of Bernoullian statistics, and then test which peak should be assigned to *mr* or *rr*. The f_{mr} values calculated in this way were 48.6% and 33.4% at 0 and −90 °C, respectively. In contrast, the calculated f_{rr} values were 17.4% and 4.5% at 0 and −90 °C, respectively. A comparison of these calculated values with those directly obtained through the deconvolution of the peaks listed in Table 1, allowed for the middle peak and the peak at the highest magnetic field to be assigned to the *mr* and *rr* triads, respectively, as shown in the upper left panel of Fig. 1.

The conditional probabilities for P_m and P_r, (i.e., the so-called first order Markovian-statistics parameters, such as $P_{r/m}$ and $P_{m/r}$) are also summarized in Table 1. For these parameters, the subscripted tacticity symbol to the left of the slash represents the added condition of the stereochemistry at the second diad from the propagating chain end, whereas the subscripted tacticity symbol to the right of the slash represents the stereochemistry of the newly formed radical immediately after the propagating reaction. For example, the parameter $P_{r/m}$ denotes the probability of an *m*-addition by an *r*-ended radical (~~~*r*M•). When the polymer propagation obeys Bernoullian statistics, $P_{r/m}$ will be equal to $P_{m/m}$ and $P_{m/r}$ will be equal to $P_{r/r}$. The equivalent relation, $P_{r/m} + P_{m/r} = 1$, is a useful measure for testing the extent to which the system obeys Bernoullian statistics; the complete deviations from Bernoullian statistics result in the ($P_{r/m} + P_{m/r}$) value of either zero or two. The sums of $P_{r/m}$ and $P_{m/r}$ are listed in Table 1 and were reasonably close to unity, with any deviations from unity being within ~10% on average. These results therefore demonstrate that the stereosequences in the PVPs prepared under the conditions listed in Table 1 almost obey Bernoullian statistics; effectively confirming the afore-mentioned assignments.

We then proceeded to evaluate the precision of the quantification of the integral intensities of the three peaks assigned to *mm*, *mr* and *rr*. Fig. S1 shows the ^{1}H NMR spectra of the $CH_{2,C=O}$ (**c**) of the PVP prepared at 0 °C (Table 1, run 6), which were measured at different magnetic strengths of 9.4, 11.7 and 21.6 T, corresponding to ^{1}H resonance frequencies of 400, 500 and 920 MHz, respectively. The triad tacticities were determined by the ratio of the integral intensity for each peak to the sum of the intensities of the three peaks belonging to the *mm*, *mr* and *rr* stereosequences, and the values are shown in Fig. S1. The intensities of the different peaks were determined by peak deconvolution. The triad tacticities determined at different magnetic fields were found to be in agreement with each other within 2.3%. The differences between the tacticities determined at ^{1}H NMR frequencies of 500 and 920 MHz were within 0.7%. Based on these results, it can be concluded that the signals obtained at a ^{1}H NMR frequency of 500 MHz are sufficient for the determination of the triad tacticities of PVPs, and this frequency was therefore selected for most of the discussions in this study.

The ^{13}C NMR spectra of the PVPs with different tacticities were also recorded, and the ^{13}C NMR spectrum of the PVP prepared in toluene at 0 °C in the presence of L-EtTar was measured in D_2O at 60 °C (Fig. 2, lower panel). The spectrum of the PVP prepared in water (Supplementary Table S1, run 14) is also shown in the upper panel of Fig. 2. The intensity of the middle peak in the signals belonging to the CH_{main} (**b**) group was decreased significantly in the spectrum of the PVP prepared in toluene in the presence of L-EtTar, compared with that of the PVP prepared in water. Although the observed splitting of these signals into three peaks might induce one to intuitively assign the three peaks to *mm*, *mr* and *rr* triads, a comparison of the intensities for the polymers prepared in toluene and water suggests that these assignments cannot be made in such a simple way, because we would then need to assume an unrealistic preference for the formation of a mixture of isotactic and syndiotactic polymers or the formation of stereoblock polymers in homogeneous radical polymerizations. This therefore implies that the ^{13}C NMR spectra of the polymers could be affected by long-range stereosequences such as pentads. The simple assignment of the three CH_{main} peaks to *mm*, *mr* and *rr* triads[14] has been adopted by many researchers to date. In another assignment suggested by Dutta and Brar[17] for ^{13}C NMR spectra that had been recorded at 75 MHz in $CDCl_3$ at 50 °C, the three peaks were assigned to *mm*+*mr*, *rr* and *mr*; here the contribution of the *mr* triad stereosequence was assigned to the first and the third peaks. These assignments correspond to implicitly and partially taking the pentad stereosequences into account. However, this assignment is particularly ambiguous with respect to the quantitative determination of the triad tacticities, because it is not possible to determine the individual contributions of the *mm* and *mr* tacticities to the peak intensities.

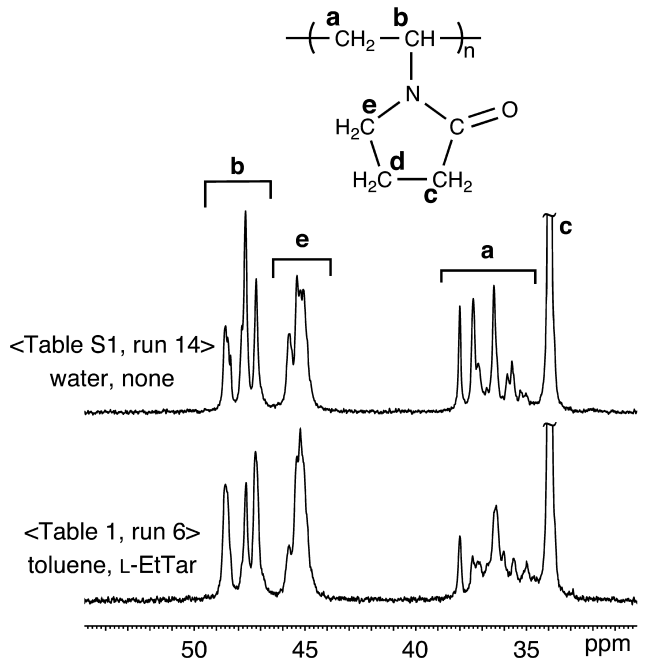

Fig. 2 100 MHz ^{13}C NMR spectra of PVPs with different tacticities, measured in D_2O at 60 °C.

Product yield and stereoregularity of PVP enhanced by L-EtTar

Table 1 summarizes the results of the radical polymerization of VP in toluene for 24 h in the presence of L-EtTar. For comparison, we have also included the results for the same experiment without the use of L-EtTar. The most remarkable effect of the addition of L-EtTar was observed in the enhancement in the polymer yield at lower temperatures. The yield per 24-h polymerization at a fixed temperature was far greater when the reaction was conducted in the presence of L-EtTar than it was for the corresponding 48-h polymerization process conducted in the absence of L-EtTar. In fact, the yields were 3.6- and 17-fold greater when the reaction was conducted at −20 and −40 °C, respectively (e.g., compare run 3 vs. run 8 and run 4 vs. run 9 in Table 1). The mechanism of the yield enhancing effect of L-EtTar could be attributed to L-EtTar effectively hindering the termination reaction.

One of the greatest advantages associated with being able to reduce the reaction temperature with the aid of L-EtTar is the wide-range control of the stereospecificity of the polymerization reaction. For example, reducing the polymerization temperature from 0 to −93 °C led to an increase in the *mm* triad content from 36.3% to 66.4% (Table 1, runs 7–13). The polymerization of VP in toluene gave product polymers that were richer in the *mm* triad, as confirmed by the reaction conducted in the absence of L-EtTar (Table 1, runs 1 and 2). This result contrasted with those of typical radical polymerization reactions, except for those of VP, where monosubstituted unconjugated monomers have been reported to produce atactic polymers almost exclusively.[9-12] It is noteworthy that the addition of L-EtTar led to a slight decrease in the *mm* triad of up to 10% compared with the reactions conducted at fixed temperatures (Table 1, runs 1 vs. 6, 2 vs. 7 and 3 vs. 8). Nevertheless, the largest fraction of *mm* triad among all of the conditions tested was obtained at the lower temperatures and in the presence of L-EtTar. These results therefore highlight the benefits of employing very low temperatures where the polymerization can only proceed following the introduction of L-EtTar.

The addition of L-EtTar also led to an increase in the molecular weights of the PVPs (Table 1, runs 1 vs. 6 and 2 vs. 7). Furthermore, the molecular weights of the PVPs prepared in the presence of L-EtTar increased slightly as the temperature of the polymerization was reduced to −60 °C (Table 1, runs 7–10). Based on this trend, it was expected that PVPs prepared at temperatures below −60 °C (Table 1, runs 11–13) would have even larger molecular weights. Unfortunately, however, the molecular weights of the polymers prepared at temperatures below −60 °C could not be determined because they were insoluble in the eluent used for SEC experiments (i.e., DMF containing 10 mmol L^{-1} LiBr). The poor solubility properties of these polymers were attributed to their higher isotacticity compared with the polymers produced at higher temperatures, because polymers with higher levels of stereoregularity are generally less soluble, as evidenced for several other polymers, including poly(*N*,*N*-dialkylacrylamide)s and poly(*N*-alkylacrylamide)s.[39-42] The average lengths of the *m* diad ($\overline{n}_m$) were calculated with $\overline{n}_m = (f_{mm} + f_{mr}/2)/(f_{mr}/2)$.[43] The threshold $\overline{n}_m$ value of ~4 can be used as a rule of thumb for assessing the solubility of PVP for the purpose of SEC.

Analysis of isotactic specificity at low temperatures in terms of overall activation energies

The mechanism leading to the stereoregular PVP was then considered in greater detail using a simple transition-state model. The difference in the activation Gibbs free energies ($G^{\ddagger}$) for isotactic and syndiotactic propagation, which governs the

Table 2. Activation parameters for radical polymerization of unconjugated monomers in toluene

Monomer	Added agent	Solvent	Temperature °C	$\frac{\Delta H_i^{\ddagger}-\Delta H_s^{\ddagger}}{\text{kJ mol}^{-1}}$	$\frac{-T(\Delta S_i^{\ddagger}-\Delta S_s^{\ddagger})}{\text{kJ mol}^{-1}}$	$\frac{\Delta G_i^{\ddagger}-\Delta G_s^{\ddagger}}{\text{kJ mol}^{-1}}$	Ref.
VP	L-EtTar	Toluene	–90	–4.1±0.2	2.0±0.2	–2.1±0.4	This work
m-ended radical			–90	–4.7±0.2	2.8±0.2	–2.0±0.4	This work
r-ended radical			–90	–4.0±0.3	1.3±0.2	–2.8±0.5	This work
VP	L-EtTar	Toluene	–40		2.5±0.2	–1.6±0.4	This work
m-ended radical			–40		3.5±0.3	–1.2±0.5	This work
r-ended radical			–40		1.6±0.3	–2.4±0.5	This work
NVA	none	Toluene	–40	–1.1±1.2	1.1±1.1	0.0±2.3	10
NVA	L-EtTar	Toluene	–40	–3.2±0.6	1.8±0.6	–1.5±1.2	10
VAc	none	Bulk	–40	0.0±0.1	0.3±0.1	0.2±0.1	9
VAc	none	$(CF_3)_3COH$	–40	2.4±0.2	–0.9±0.2	1.4±0.3	9

stereoselectivity between the *m* and *r* diads, can be separated into the contributions of the activation enthalpy ($H^{\ddagger}$) and activation entropy ($S^{\ddagger}$) terms using Fordham's plots, as shown in Fig. 3. The plots can be fitted to an Arrhenius-type function, which can be expressed as follows:[44]

$$\ln\left(\frac{P_m}{P_r}\right) = -\frac{\Delta H_i^{\ddagger} - \Delta H_s^{\ddagger}}{RT} + \frac{\Delta S_i^{\ddagger} - \Delta S_s^{\ddagger}}{R} \quad (1)$$

where the i and s subscripts denote the isotactic and syndiotactic propagations, respectively. A large value for the probability ratio P_m/P_r together with a negative value for $\Delta G_i^{\ddagger} - \Delta G_s^{\ddagger}$ corresponds to a high isotactic selectivity. Because the current polymer satisfactorily obeys Bernoullian statistics, the probabilities P_m and P_r for the single-unit propagation can be regarded as being the same as the fractions f_m and f_r. The fractions f_m and f_r were calculated from the triad tacticities, which were determined directly from the ^{1}H NMR spectra (Table 1) using the following simple relations: $f_m = f_{mm} + f_{mr}/2$ and $f_r = f_{rr} + f_{mr}/2$.

The difference in the Gibbs free energy, $\Delta G_i^{\ddagger} - \Delta G_s^{\ddagger}$, revealed a negative value of -2.1 ± 0.4 kJ mol^{-1} for the VP polymerization reaction conducted in the presence of L-EtTar at −90 °C (Table 2). This large negative value for $\Delta G_i^{\ddagger} - \Delta G_s^{\ddagger}$ occurred as a consequence of an even more negative value of $\Delta H_i^{\ddagger} - \Delta H_s^{\ddagger}$. The entropy term, $-T(\Delta S_i^{\ddagger} - \Delta S_s^{\ddagger})$, was positive and in favor of the syndiotactic specificity. Nevertheless, the enthalpy term overwhelmed the entropy term, which resulted in the Gibbs free energy term being significantly in favor of isotactic specificity.

The probability ratios for the *m*-ended ($P_{m/m}/P_{m/r}$) and *r*-ended ($P_{r/m}/P_{r/r}$) radicals were also plotted, as shown in Fig. 3. The signs and the slopes for $P_{m/m}/P_{m/r}$ and $P_{r/m}/P_{r/r}$ against the inverse temperature were both common and close to those of P_m/P_r. These similarities were attributed to the current PVP roughly following Bernoullian statistics. Any moderate deviation from P_m/P_r could be viewed as a manifestation of the minor effect of the first-order Markovian statistics. The $\Delta G_i^{\ddagger} - \Delta G_s^{\ddagger}$ value was more largely negative for the *r*-ended radical than that of the *m*-ended radical. This difference between the *r*- and *m*-ended radicals was predominantly attributed to difference in the entropy terms for the *r*- and *m*-ended radicals, which were 1.3 ± 0.2 and 2.8 ± 0.2 kJ mol^{-1}, respectively, at −90 °C (Table 2). The largely positive value of the entropy term for the *m*-ended radical, which corresponds to a smaller $\Delta S_i^{\ddagger}$ value relative to the $\Delta S_s^{\ddagger}$ value, suggested that the *m*-addition by the *m*-ended radical required a decrease in the number of degrees of freedom in the activation state. The most likely explanation for such a decrease in the number of degrees of freedom could be the formation of "helical" conformations close to the end of the chain, which could be induced by the bulky tartrates binding to the carbonyl groups. In fact, for polymer propagation in the isotactic fashion, helical conformation is typically proposed for methacrylic monomers bearing bulky side chains, such as triphenylmethyl methacrylate[45] and *N*-triphenylmethylmethacrylamide.[46] Furthermore, although the helical conformation would entropically disfavor the formation of an *mm* triad, the Gibbs free energy was in favor of the *mm* triad because of the dominating contribution of the enthalpy term. The enthalpy term was more highly negative for the *m*-ended radical than it was for the *r*-ended radical, most likely because the helical conformation would enable the neighboring bulky side chains to avoid any sterically-induced repulsive interactions.

The activation parameters were compared with those of two other polymerizations, in which stereospecificity was induced by L-EtTar or an alcohol solvent, to develop a deeper understanding of the molecular basis for the observed stereospecificity. These comparisons were made at −40 °C, which was the lowest common temperature for the three different polymerizations being considered. The $\Delta G_i^{\ddagger} - \Delta G_s^{\ddagger}$ value was found to be negative for the NVA polymerization[10] conducted in the presence of L-EtTar, which was similar to the result observed for PVP. In contrast to these two polymerization reactions, the $\Delta G_i^{\ddagger} - \Delta G_s^{\ddagger}$ value for the vinyl acetate (VAc) polymerization[9] was positive in nonafluoro-*tert*-butanol ($(CF_3)_3COH$). This difference in the signs of the polymers was attributed to differences in their enthalpy contributions, with the enthalpy favoring the *r* diad for VAc and the *m* diad for the other polymers. Furthermore, the enthalpy term made the greatest contribution to the Gibbs free energy of all of the polymers considered in this comparison. The order of the absolute values of the $\Delta H_i^{\ddagger} - \Delta H_s^{\ddagger}$ and $-T(\Delta S_i^{\ddagger} - \Delta S_s^{\ddagger})$ terms for the three polymerizations were of the order VP > NVA > VAc. The absolute values of the $\Delta G_i^{\ddagger} - \Delta G_s^{\ddagger}$ terms for the three polymerizations were similar because of the partial cancellation of the enthalpy and entropy terms for each polymerization. These differences between the polymerizations can therefore be attributed to differences in the size and conformational freedom properties of the side chain structures of the monomers (i.e., cyclic amide in VP, acyclic amide in NVA and acyclic ester in VAc). For the polymerization conditions containing no tartrate or alcohol solvent (i.e., the NVA polymerization in neat toluene and the VAc polymerization conducted in the bulk VAc), the $\Delta G_i^{\ddagger} - \Delta G_s^{\ddagger}$ values were almost zero in both cases, which resulted in the formation of atactic polymers. These results therefore further highlighted the importance of the tartrates to the stereoselectivity of the polymerization process.

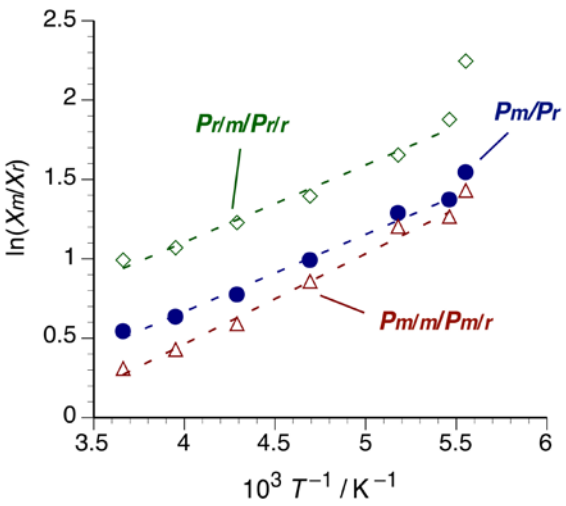

Fig. 3 Fordham's plots of P_m/P_r, $P_{m/m}/P_{m/r}$ and $P_{r/m}/P_{r/r}$ for the VP polymerization in toluene at low temperatures in the presence of L-EtTar. The data at −93 °C have been excluded from the linear fitting (dashed lines) to obtain the activation parameters.

Hydrogen-bonding interactions between VP and L-EtTar

To develop a deeper understanding of why the addition of L-EtTar led to such a dramatic increase in the yield of PVP, we investigated the formation of hydrogen-bonding interactions between the VP monomer and L-EtTar by examining changes in the ^{13}C NMR spectra of VP and L-EtTar following their mixing. Fig. 4 shows the ^{13}C NMR spectra of the C=O carbons in an equimolar mixture of VP and L-EtTar in toluene-d_8 at −60 °C. The ^{13}C chemical shifts of VP and L-EtTar were highly sensitive to the formation of hydrogen bonds between these two species, which led to significant changes in their intra- and intermolecular electron distributions. The signal belonging to the amide C=O carbon of the VP monomer showed a large downfield shift of 1.15 ppm when it was mixed with L-EtTar. In contrast, the signal belonging to the ester C=O carbon in L-EtTar showed an upfield shift of 0.27 ppm following its mixing with VP. This upfield shift in the signals belonging the ester C=O carbons in L-EtTar was attributed to the reorganization of the hydrogen bonds from those associated with the self-aggregation of L-EtTar, which formed between the ester C=O and hydroxyl groups of L-EtTar, to the formation of hydrogen bonds between VP and L-EtTar. In contrast, the large downfield shift was observed for the C=O carbon of VP, suggested that this group had formed two hydrogen bonds. These results were consistent with our previous study on DMAAm, where the formation of a 1:1 complex with tartrate occurred through a double hydrogen-bonding interactions, which was confirmed by the examination of the maximum position of the Job's plot.[25] The ^{1}H NMR spectra of VP, L-EtTar and an equimolar mixture of these two components are shown in Fig. S2. The signal for the hydroxyl group (**E**) of L-EtTar exhibited a downfield shift. Furthermore, the down-field-shifted signals of the methine protons (**C**) in L-EtTar were split into two signals when this material was mixed with VP. This splitting most likely occurred as a consequence of the coupling between the methine protons and the hydroxyl protons, because the chemical exchange of these protons would be restricted following the formation of the hydrogen bonds.

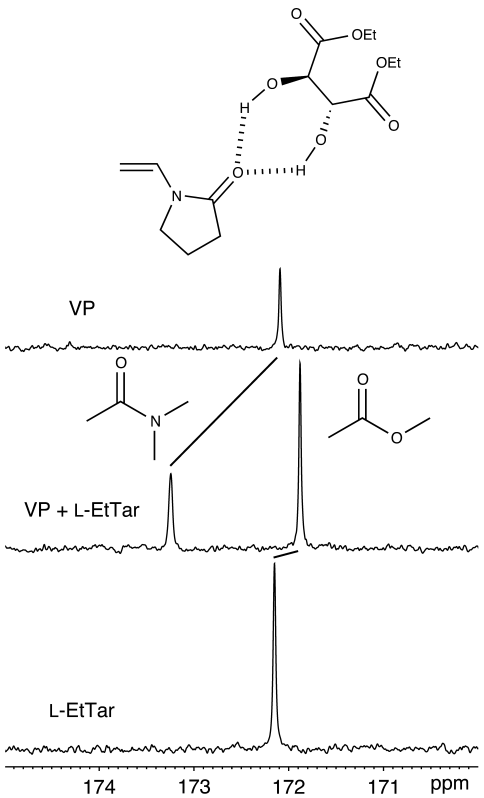

Fig. 4 100 MHz ^{13}C NMR spectra of the carbonyl carbons of VP (0.1 mol L^{-1}), L-EtTar (0.1 mol L^{-1}) and an equimolar mixture of these two components (0.1 mol L^{-1} for each). These spectra were measured in toluene-d_8 at −60 °C.

These results corroborate the formation of a complex between VP and L-EtTar, which would be stabilized by double hydrogen bonds in a similar manner to those previously reported for the NVA-tartrate[10] and DMAAm-tartrate[25] complexes. The formation of this complex would therefore allow for the successful preparation of isotactic-rich PVPs via a radical polymerization reaction at low temperatures. The mechanism for the yield enhancement could be explained in terms of the termination step being hindered by the formation of the double hydrogen-bonding interaction. The proposed mechanism for the termination reaction is illustrated in Scheme S1. According to this scheme, termination would be achieved by the bimolecular interaction of the propagating radicals. The propagating radical species would therefore become sterically more encumbered when it formed a hydrogen-bonding complex with L-EtTar, which would prevent close contact between the reactive sites and prevent the two bulky propagating radicals from undergoing the terminating reaction.

High-resolution ^{1}H NMR measurement for PVP

High-temperature measurement. High temperature NMR measurements provide a powerful approach for improving the spectral resolution and peak separation of polymers by taking advantage of the motional narrowing at elevated temperatures.[38] The polymers synthesized in the current study were subjected to high-temperature NMR measurements using the specially-designed NMR probe.[29] In this particular study, we

were interested in assessing the extent to which the peaks for the polymers become narrower as a result of the enhanced molecular motions at high temperatures. ^{1}H NMR spectra were obtained at temperatures ranging from 5 to 250 °C in three different solvents, including $CDCl_3$, DMSO-d_6 and D_2O. Of the three solvents tested, the most significant spectral changes following increases in the temperature elevation were observed in D_2O. The spectra obtained at different temperatures in D_2O are shown in Fig. 5.

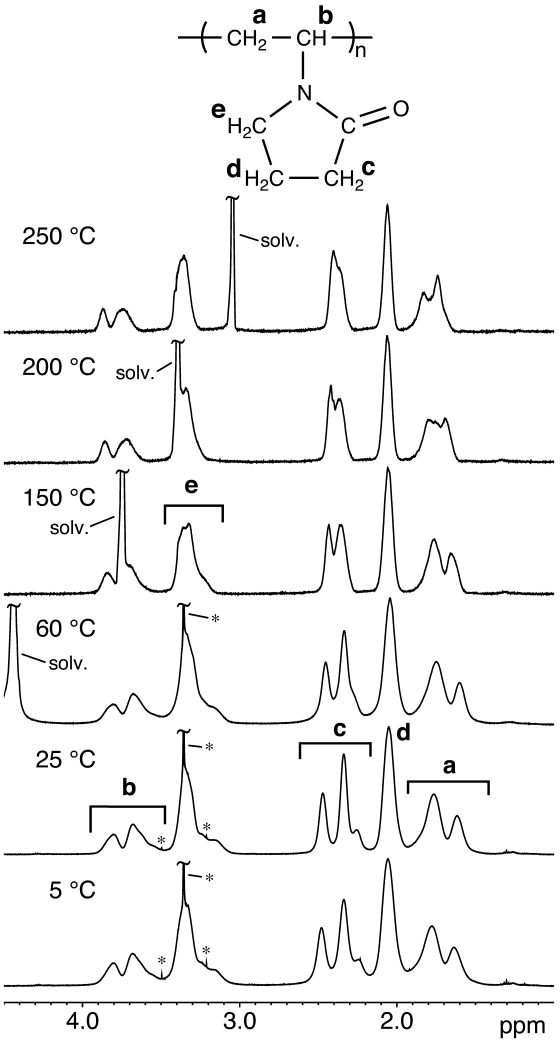

Fig. 5 500 MHz ^{1}H NMR spectra of PVPs in D_2O at temperatures in the range of 5–250 °C (Table 1, run 6, 2.0 wt%). The asterisk (*) denotes impurities. The spectra at 5–60 °C and 150–250 °C were recorded using standard and high-temperature probes, respectively.

The most noticeable temperature dependence was observed for the signals of the $CH_{2,C=O}$ (**c**) groups. The signals of $CH_{2,C=O}$ (**c**) groups showed clear three-line splitting at temperatures below 60 °C. Increasing the temperature to 250 °C led to a significant narrowing in the width of each split peak. The peak positions and intensities varied with temperature, with the three peaks observed at lower temperatures appearing to coalesce into two peaks at higher temperatures. The narrowing of the peaks with temperature was also observed for the signals of the $CH_{2,main}$ (**a**) and CH_{main} (**b**) groups.

Factors leading to the observed changes in the shape of the signal for the $CH_{2,C=O}$ (**c**) groups can be summarized as follows. The narrowing of the peak widths occurred as expected at high temperatures because of the accelerated kinetic motions. The apparent coalescence of three peaks into two peaks reflects the enhanced random side-chain (and possibly main-chain) motions, which would make it difficult to distinguish the different stereosequences from each other. Furthermore, the separation between the two dominant peaks, which were assigned as the *mm* and *mr* triads, would become smaller with increasing temperature, as shown in Fig. S3. This reduction in the separation between the two dominant peaks would most likely occur as a consequence of motional narrowing and fluctuations in the chemical shifts, which would be controlled by the temperature-dependent state of the hydrogen bonding between the C=O groups and the solvent D_2O molecules. These competing factors would therefore result in the remarkable simplification of the NMR spectra at a subcritical temperature of 250 °C.

The spectra in the other two solvents $CDCl_3$ and DMSO-d_6 are shown in Figs. S4 and S5, respectively. In $CDCl_3$, the spectral patterns changed slightly when the temperature was increased from 150 to 200 °C, as shown in Fig. S4. New signals appeared at 1.22, 1.35 and 2.88 ppm when the ^{1}H NMR in $CDCl_3$ was recorded at 250 °C. When the sample tube was taken out of the NMR apparatus after the measurement at 250 °C, the PVP solution in $CDCl_3$ had become slightly brown in color and some of the PVP had precipitated from the solution. In contrast, the sample solution remained colorless when the D_2O was used as the solvent for the NMR analysis at 250 °C and the PVP remained in solution. These observations suggested that the PVP was decomposing and/or undergoing some type of cross-linking reaction in $CDCl_3$ at 250 °C. In DMSO-d_6, the PVP solution became slightly colored following the high-temperature NMR measurement at 250 °C, although the PVP material remained dissolved in solution. The signals for the $CH_{2,C=O}$ (**c**) group showed an obvious temperature dependence in DMSO-d_6, which was similar to that observed in D_2O (Fig. S5). The chemical-shift separation between the peaks for the *mm* and *mr* triads was larger in DMSO-d_6 than it was in D_2O over the whole range of temperatures investigated (Fig. S3). Despite this larger separation in DMSO-d_6, D_2O was selected as the best solvent for the determination of the triad fractions, because the peaks for the *mr* and *rr* triads in DMSO-d_6 overlapped with the signals of the middle methylene groups (**d**) of the trimethylene groups of the side chain. More importantly, the narrowing effect on the peak widths realized by temperature elevation was far larger than those obtained by the choice of solvent or decreasing the polymer concentration, as seen in Fig. S3.

It is noteworthy that the $CH_{2,C=O}$ (**c**) group exhibited the largest temperature change, even though this group was three bond lengths and therefore the furthest distance away from the stereogenic center (site **b**). A similar tendency was also observed for poly(methyl methacrylate),[38] where the signals belonging to the methoxy groups, which were three bond lengths and therefore the furthest away from the stereogenic centers, exhibited a larger temperature dependence than those of the α-methyl groups, which were directly attached to the stereogenic centers, when measured in aromatic solvents such as benzene.

Optimal conditions for the measurement of the peak separation/resolution. The effects of the NMR measurement conditions (i.e., temperature and static-magnetic-field strength) were also investigated, in terms of their impact on the separation and resolution of the peaks for triad stereosequences, to determine the optimal conditions for the NMR measurements. The extent to which the peaks were separated was evaluated on the basis of what we call the peak separation/resolution criteria. To measure the separation and resolution properties of the neighboring peaks A and B, we used the ratio of the height of the valley point to the average of the heights of the two peaks according to the following formula: $\Phi_{A\text{-}B} = H_{A\text{-}B}/[(H_A + H_B)/2]$, where $H_{A\text{-}B}$ denotes the height of the valley point between peaks A and B, and H_A and H_B denote the heights of peaks A and B, respectively. These definitions are illustrated in Fig. S6. By definition, the Φ value is bounded between zero and unity, where the Φ values of zero and unity correspond to complete base-line separation and the complete overlap of the two peaks, respectively.

The dependence of Φ on the measurement temperature is plotted in Fig. 6. At temperatures in the range of 5 to 40 °C, both $\Phi_{mr\text{-}rr}$ and $\Phi_{mm\text{-}mr}$ decreased with increasing temperature, most likely because the broadening of the peak at the lower temperatures was reduced with the temperature increment. At temperatures greater than 60 °C, it was only possible to evaluate Φ for the *mm*-*mr* pair because the *rr* peak merged into the *mr* peak above 60 °C, as shown in Fig. 5. The temperature dependence of $\Phi_{mm\text{-}mr}$ turned over at ~40 °C and the Φ value then increased with increasing temperature. The $\Phi_{mr\text{-}rr}$ also reached a minimum at 25–40 °C. It was therefore concluded that the peak separation/resolution was optimized at temperatures in the range of 25–40 °C.

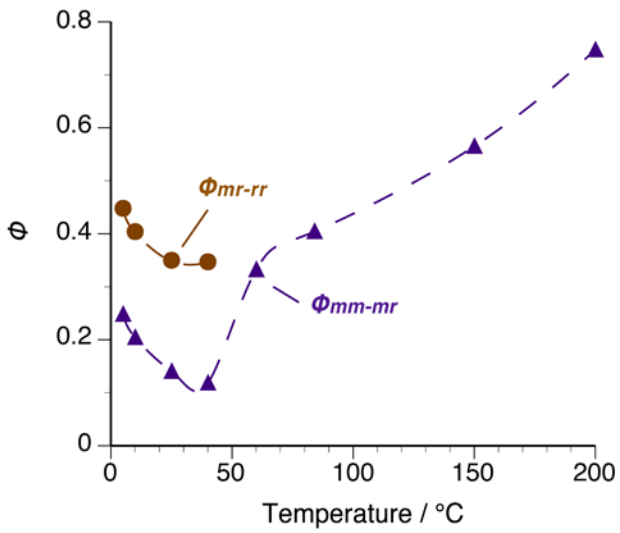

Fig. 6 Temperature dependences of the $\Phi_{mm\text{-}mr}$ and $\Phi_{mr\text{-}rr}$ values from the 500 MHz ^{1}H NMR spectra of PVP (Table 1, run 6) in D_2O.

The Φ values for the PVPs with different tacticities were also plotted against temperature, and these plots are shown in Fig. S7. The $\Phi_{mr\text{-}rr}$ values were heavily dependent on the tacticity of the PVPs, whereas the $\Phi_{mm\text{-}mr}$ values were almost independent of the tacticity. This difference was attributed to the peaks assigned to the *mr* triad overlapping to a much greater extent with those of the *rr* triad than the *mm* triad. The $\Phi_{mr\text{-}rr}$ showed a minimum at 25 °C for runs 14 and 15, and it was therefore decided that 25 °C was the optimum temperature for determining the tacticities of the PVPs based on their ^{1}H NMR spectra.

The extent to which recording the NMR measurements at a higher magnetic field could improve the peak separations was also investigated. A comparison of the ^{1}H NMR spectra of the PVPs obtained at 400, 500 and 920 MHz is shown in Fig. S1. The Φ values were plotted against the magnetic field, and the results are shown in Fig. 7. This plot clearly shows that the peak separation/resolution improved with increasing magnetic field strength. In particular, the $\Phi_{mr\text{-}rr}$ value at 920 MHz was reduced to the same level as the $\Phi_{mm\text{-}mr}$ value at 400 MHz. Although a ^{1}H NMR frequency of 500 MHz was completely satisfactory for the quantitative discussions provided in the current study, the use of ultra-high-field NMR would be highly beneficial for polymer samples requiring extensive peak deconvolution processes, such as syndiotactic-rich PVPs, which will be investigated in detail as part of our future work.

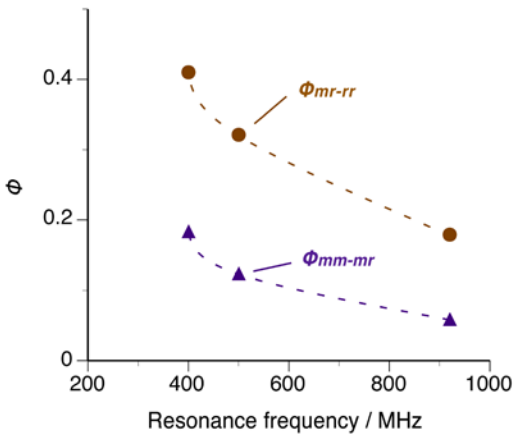

Fig. 7 Relationship between the $\Phi_{mm\text{-}mr}$ and $\Phi_{mr\text{-}rr}$ values and the resonance frequency in the ^{1}H NMR spectra of PVP (Table 1, run 6, in D_2O at 25 °C, 1.0 wt%).

Conclusions

The effect of L-EtTar on the radical polymerization of VP in toluene at low temperatures has been investigated. The addition of L-EtTar led to dramatic improvements in the PVP yield, most likely because of its ability to inhibit the terminating reaction through steric hindrance arising from the formation of a hydrogen-bonded complex. Furthermore, the isotacticity of the PVP increased as the polymerization temperature decreased, and PVP with an *mm* value of 66.4% was obtained at the lowest temperature studied of −93 °C. To the best of our knowledge, this work therefore represents the first reported example of the synthesis of isotactic-rich PVP.

The optimal conditions for the ^{1}H NMR measurement of PVP were determined following a series of screening experiments and we subsequently succeeded in assigning the $CH_{2,C=O}$ signal split into three peaks. These new ^{1}H assignments allowed us to establish a methodology for determining the different fractions of the triad stereosequences for PVPs. The NMR-measurement temperature that gave the best peak separation was determined to be in the vicinity of room temperature. High-temperature NMR measurements showed that the signals coalesced and that the spectra were dramatically simplified in hot water at 250 °C. This result

encouraged us to apply high-temperature NMR methods to polymers whose spectra were too complicated to be deconvoluted by means of conventional procedures (e.g., copolymers). Our future work in this area will focus on the development of methods for determining monomer reactivity ratios from a single copolymer sample.[47]

Acknowledgements

This work was supported in part by KAKENHI [a Grant-in-Aid for Young Scientists (B) (23750130) (TH) and a Grant-in-Aid for Scientific Research (C) (25410019) (KY)] and the JGC-S Scholarship Foundation (TH). The authors are grateful to the Institute for Molecular Science, Japan, for the 920 MHz ^{1}H NMR measurements. The authors are grateful to Professors Yasuhiro Uosaki and Masaru Nakahara for many fruitful discussions about the high-temperature NMR method used in the current study.

Department of Chemical Science and Technology, Institute of Technology and Science, The University of Tokushima, Minamijosanjima 2-1, Tokushima 770-8506, Japan. E-mail: hirano@chem.tokushima-u.ac.jp

Electronic Supplementary Information (ESI) available: Additional ^{1}H NMR spectra including those at 920 MHz, high-temperature ^{1}H NMR spectra in $CDCl_3$ and DMSO-d_6 and the temperature dependencies of the chemical shift values for $CH_{2,C=O}$ peaks in the two solvents, the definition of the $\Phi_{mm\text{-}mr}$ and $\Phi_{mr\text{-}rr}$ values; Scheme for the proposed mechanism of the terminating reaction; Table for PVPs with different stereoregularities. See DOI: 10.1039/b000000x/

Notes and references

1. F. Haaf, A. Sanner and F. Straub, *Polym. J.*, 1985, 17, 143-152.
2. F. Fischer and S. Bauer, *Chem. unserer Zeit*, 2009, 43, 376-383.
3. M. J. O'Connell, P. Boul, L. M. Ericson, C. Huffman, Y. Wang, E. Haroz, C. Kuper, J. Tour, K. D. Ausman and R. E. Smalley, *Chem. Phys. Lett.*, 2001, 342, 265-271.
4. M. Hamidi, A. Azadi and P. Rafiei, *Adv. Drug Del. Rev.*, 2008, 60, 1638-1649.
5. B. Lim, M. Jiang, J. Tao, P. H. C. Camargo, Y. Zhu and Y. Xia, *Adv. Funct. Mater.*, 2009, 19, 189-200.
6. B. Le Droumaguet and J. Nicolas, *Polym. Chem.*, 2010, 1, 563-598.
7. R. Fukae, K. Kawakami, T. Yamamoto, O. Sangen, T. Kako and M. Kamachi, *Polym. J.*, 1995, 27, 1257-1259.
8. K. Imai, T. Shiomi, N. Oda and H. Otsuka, *J. Polym. Sci., Part A: Polym. Chem.*, 1986, 24, 3225-3231.
9. K. Yamada, T. Nakano and Y. Okamoto, *Macromolecules*, 1998, 31, 7598-7605.
10. T. Hirano, Y. Okumura, M. Seno and T. Sato, *Eur. Polym. J.*, 2006, 42, 2114-2124.
11. T. Uemura, Y. Ono, K. Kitagawa and S. Kitagawa, *Macromolecules*, 2007, 41, 87-94.
12. H. Ajiro and M. Akashi, *Macromolecules*, 2009, 42, 489-493.
13. K. Satoh and M. Kamigaito, *Chem. Rev.*, 2009, 109, 5120-5156.
14. H. N. Cheng, T. E. Smith and D. M. Vitus, *J. Polym. Sci.: Polym. Lett. Ed.*, 1981, 19, 29-31.
15. J. R. Ebdon, T. N. Huckerby and E. Senogles, *Polymer*, 1983, 24, 339-343.
16. G. W. Busser, J. G. van Ommen and J. A. Lercher, *J. Phys. Chem. B*, 1999, 103, 1651-1659.
17. K. Dutta and A. S. Brar, *J. Polym. Sci., Part A: Polym. Chem.*, 1999, 37, 3922-3928.
18. T. J. Carver, M. G. B. Drew and P. M. Rodger, *Ann. N.Y. Acad. Sci.*, 2000, 912, 658-668.
19. T.-X. Xiang and B. D. Anderson, *J. Pharm. Sci.*, 2004, 93, 855-876.
20. T.-X. Xiang and B. D. Anderson, *Pharm. Res.*, 2005, 22, 1205-1214.
21. D. Wan, K. Satoh, M. Kamigaito and Y. Okamoto, *Macromolecules*, 2005, 38, 10397-10405.
22. T. Hirano, Y. Okumura, H. Kitajima, M. Seno and T. Sato, *J. Polym. Sci., Part A: Polym. Chem.*, 2006, 44, 4450-4460.
23. T. Hirano, T. Miyazaki and K. Ute, *J. Polym. Sci., Part A: Polym. Chem.*, 2008, 46, 5698-5701.
24. T. Hirano, T. Kamikubo, Y. Okumura, Y. Bando, R. Yamaoka, T. Mori and K. Ute, *J. Polym. Sci., Part A: Polym. Chem.*, 2009, 47, 2539-2550.
25. T. Hirano, S. Masuda, S. Nasu, K. Ute and T. Sato, *J. Polym. Sci., Part A: Polym. Chem.*, 2009, 47, 1192-1203.
26. T. Hirano, T. Kamikubo and K. Ute, *Polym. Int.*, 2012, 61, 966-970.
27. T. Hirano, S. Masuda and T. Sato, *J. Polym. Sci., Part A: Polym. Chem.*, 2008, 46, 3145-3149.
28. W. Liu, T. Nakano and Y. Okamoto, *Polym. J.*, 2000, 32, 771-777.
29. K. Yoshida, C. Wakai, N. Matubayasi and M. Nakahara, *J. Chem. Phys.*, 2005, 123, 164506.
30. K. Yoshida, N. Matubayasi and M. Nakahara, *J. Chem. Phys.*, 2006, 125, 074307.
31. K. Yoshida, N. Matubayasi and M. Nakahara, *J. Chem. Phys.*, 2008, 129, 214501.
32. K. Yoshida, N. Matubayasi and M. Nakahara, *J. Mol. Liq.*, 2009, 147, 96-101.
33. K. Yoshida, N. Matubayasi, Y. Uosaki and M. Nakahara, *J. Chem. Eng. Data*, 2010, 55, 2815-2823.
34. Z. Zhang and T. C. M. Chung, *Macromolecules*, 2006, 39, 5187-5189.
35. The conventional calibration procedure with polystyrene standards we employed here is sufficiently precise for the present purpose of the rough relative comparison of the effect of the addition of L-EtTar because, as listed in Table 1, the differences observed between the polymers synthesized in the presence and absence of L-EtTar far exceed the technical uncertainties of the conventional SEC method. Further details of the calibration procedures of SEC were described in Refs. 36 and 37.
36. M. Netopilík and P. Kratochvíl, *Polymer*, 2003, 44, 3431-3436.
37. Y. Guillaneuf and P. Castignolles, *J. Polym. Sci., Part A: Polym. Chem.*, 2008, 46, 897-911.
38. K. Hatada and T. Kitayama, *NMR spectroscopy of polymers*, Springer-Verlag, Berlin, 2004.
39. K. Butler, P. R. Thomas and G. J. Tyler, *J. Polym. Sci.*, 1960, 48, 357-366.
40. M. Kobayashi, S. Okuyama, T. Ishizone and S. Nakahama, *Macromolecules*, 1999, 32, 6466-6477.
41. B. Ray, Y. Okamoto, M. Kamigaito, M. Sawamoto, K.-i. Seno, S. Kanaoka and S. Aoshima, *Polym. J.*, 2005, 37, 234-237.
42. T. Hirano, A. Ono, H. Yamamoto, T. Mori, Y. Maeda, M. Oshimura and K. Ute, *Polymer*, 2013, 54, 5601-5608.
43. J. C. Randall, *Macromolecules*, 1978, 11, 592-597.
44. J. W. L. Fordham, *J. Polym. Sci.*, 1959, 39, 321-334.
45. T. Nakano, A. Matsuda and Y. Okamoto, *Polym. J.*, 1996, 28, 556-558.
46. N. Hoshikawa, Y. Hotta and Y. Okamoto, *J. Am. Chem. Soc.*, 2003, 125, 12380-12381.
47. R. Chujo, H. Ubara and A. Nishioka, *Polym. J.*, 1972, 3, 670-674.